Cavity enhanced spin measurement of the ground state spin of an NV center in diamond

2009 New J. Phys. 11 013007

(http://iopscience.iop.org/1367-2630/11/1/013007)

New Journal of Physics
The open-access journal for physics

Cavity enhanced spin measurement of the ground state spin of an NV center in diamond

A Young[1], C Y Hu, L Marseglia, J P Harrison, J L O'Brien and J G Rarity

Department of Electrical and Electronic Engineering, University of Bristol, University Walk, Bristol BS8 1TR, UK
E-mail: A.Young@bristol.ac.uk

New Journal of Physics **11** (2009) 013007 (9pp)
Received 25 June 2008
Published 7 January 2009
Online at http://www.njp.org/
doi:10.1088/1367-2630/11/1/013007

Abstract. A key step in the use of diamond nitrogen vacancy (NV) centers for quantum computational tasks is a single shot quantum non-demolition measurement of the electronic spin state. Here, we propose a high fidelity measurement of the ground state spin of a single NV center, using the effects of cavity quantum electrodynamics. The scheme we propose is based in the one-dimensional atom or Purcell regime, removing the need for high Q cavities that are challenging to fabricate. The ground state spin of the NV center has a splitting of $\approx$6–10 μeV, which can be resolved in a high-resolution absorption measurement. By incorporating the center in a low-Q and low volume cavity we show that it is possible to perform single shot readout of the ground state spin using a weak laser with an error rate of $\approx 7 \times 10^{-3}$, when realistic experimental parameters are considered. Since very low levels of light are used to probe the state of the spin we limit the number of florescence cycles, which dramatically reduces the measurement induced decoherence approximating a non-demolition measurement of ground state spin.

Addressing single spins is an important route to quantum computation [1]. The long decoherence times of spins such as trapped atoms [2, 3], ions [4], or charged quantum dots [5], make them ideal candidates for storing and processing quantum information. There are many schemes for using internal spin states in all these architectures [4, 6, 7], resulting in the demonstration of fundamental quantum logic gates [8]–[10]. Nitrogen vacancy (NV) centers in diamond have long decoherence times even at room temperature [11] making them another

[1] Author to whom any correspondence should be addressed.

promising candidate for performing quantum information tasks. Several experiments have shown the manipulation of the ground state spin of a diamond NV center using optically detected magnetic resonance (ODMR) techniques [11, 12]. This has further led to the coherent control of single ^{13}C nuclear spins and quantum logic operations [13, 14]. The main problem in using ODMR is that the detection step involves observing fluorescence cycles from the NV center, which has a probability of destroying the spin memory. Since the energy level transitions of the NV center are not polarization sensitive, we cannot use Faraday rotations to perform quantum non-demolition measurements of the spin state as was shown for charged quantum dots [15, 16]. The scheme we propose here is similar to the ODMR scheme, however, by the introduction of a low Q cavity we vastly reduce the number of photons required to probe the spin state, therefore keeping the disturbance of the ground state spin to a minimum and not destroying the spin memory. Although in this paper we specialize to the NV center this scheme is applicable to any atomic or molecular system with resolvable transitions.

If we consider the energy level structure of the NV center in figure 1 (exact splittings can vary in different crystal field, normally this will not affect our final results). The ground state is a spin triplet split by 2.88 GHz due to spin–spin interactions [18]. The excited state is a triplet split by spin–spin interactions, but with the further addition of spin–orbit coupling [20]. Recent experimental evidence [17] has uncovered this excited state structure (figure 1). The net effect of spin–spin and spin–orbit interactions is to create a detuning $\approx$1.4 GHz (6 μeV) between the transitions $^3\mathrm{A}_{(m=0)} \rightarrow {}^3\mathrm{E}$ and $^3\mathrm{A}_{(m=+1)} \rightarrow {}^3\mathrm{E}$. A similar detuning of $\approx$2.5 GHz (10 μeV) exists for the $^3\mathrm{A}_{(m=-1)} \rightarrow {}^3\mathrm{E}$ transition. It is these detunings that we plan to exploit to measure the ground state spin of the defect. The energy level structure is not simply a ground and excited triplet state, there also exists an intermediate singlet state ^{1}A. There is a probability of the transition $^3\mathrm{E} \rightarrow {}^1\mathrm{A}$, with different rates depending on the spin. For the $^3\mathrm{E}_{m=\pm1}$ states (transitions 6,7) both theoretical predictions and experimental results suggest that the decay rate is around $0.4 \times 1/\tau$ [20]–[22], where τ is the spontaneous emission (SE) lifetime ($\approx$13 ns). For the $^3\mathrm{E}_{m=0}$ state (transition 5) theoretically the rate of decay to the singlet should be zero [20], however, experimental observations have shown the rate to be $\approx 10^{-4} \times 1/\tau$ [21]. Since the ^{1}A singlet state decays preferentially to the $^3\mathrm{E}_{m=0}$ state [20, 23] (transition 8), then it is clear from the rates above that broadband excitation leads to spin polarization in the spin zero ground state [24]. Since transition 8 is non-radiative then there will be a dark period in the fluorescence when it becomes populated, and as the decay rate from $^3\mathrm{E}_{m=\pm1}$ to the singlet state is much larger than from $^3\mathrm{E}_{m=0}$, the change in intensity measures the spin state [21]. Clearly using fluorescence intensity to detect the spin state has a probability to flip the spin, therefore it would seem necessary for a scheme to suppress this. However, spin-flip transitions are essential to initialize the system. Thus a compromise is required between the perfectly cyclic spin preserving transitions required for readout, and the Λ type spin-flip transition required for initialization.

We consider the structure in figure 2, which can be modeled as a single sided cavity, where κ is the cavity decay rate (side leakage), η is the coupling of the cavity to external modes, g is the NV center cavity coupling rate and γ is the NV dipole decay rate. We can write down the Heisenberg equations of motion for this structure as [27]:

$$\frac{\mathrm{d}\hat{a}}{\mathrm{d}t} = -\left[\mathrm{i}(\omega_\mathrm{c} - \omega) + \frac{\eta}{2} + \frac{\kappa}{2}\right]\hat{a} - g\sigma_- - \sqrt{\eta}b_\mathrm{in}, \tag{1}$$

$$\frac{\mathrm{d}\sigma_-}{\mathrm{d}t} = -\left[\mathrm{i}(\omega_\mathrm{a} - \omega) + \frac{\gamma}{2}\right]\sigma_- - g\hat{\sigma}_z\hat{a}, \tag{2}$$

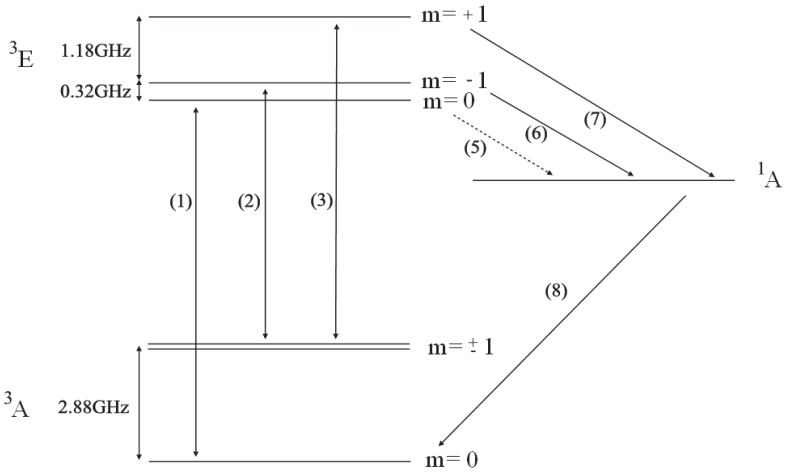

Figure 1. Experimentally measured energy level diagram of the NV center in diamond showing the experimentally determined ground and excited state splitting [17, 18]. The defect has zero phonon line at 637 nm, with width of order MHz at low temperatures [19].

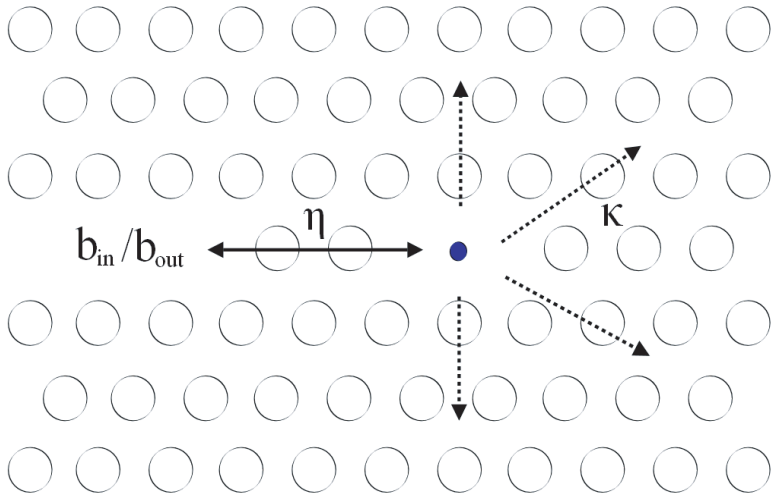

Figure 2. Schematic diagram of an NV center embedded in photonic crystal cavity with cavity decay rate κ coupled to a photonic crystal waveguide at a rate η. For two-dimensional photonic crystals suspended geometries simulations have shown Q factors larger than 10^6 for mode volumes around 0.02 μm^3, or larger than 10^5 for mode volumes around 0.008 μm^3 [25]. Experimental evidence involving coupling waveguides to similar cavities have shown efficiencies of 90% [26].

$$\frac{d\sigma_z}{dt} = \gamma(1+\sigma_z) - 2g(\sigma_-\hat{a}^\dagger + \hat{a}\sigma_+), \tag{3}$$

where ω_a and ω_c are the atomic transition (σ_-) and the intracavity photon (annihilation operator $\hat{a}$) frequencies, respectively. $\hat{\sigma}_z$ represents a Pauli Z operator on the atomic state and

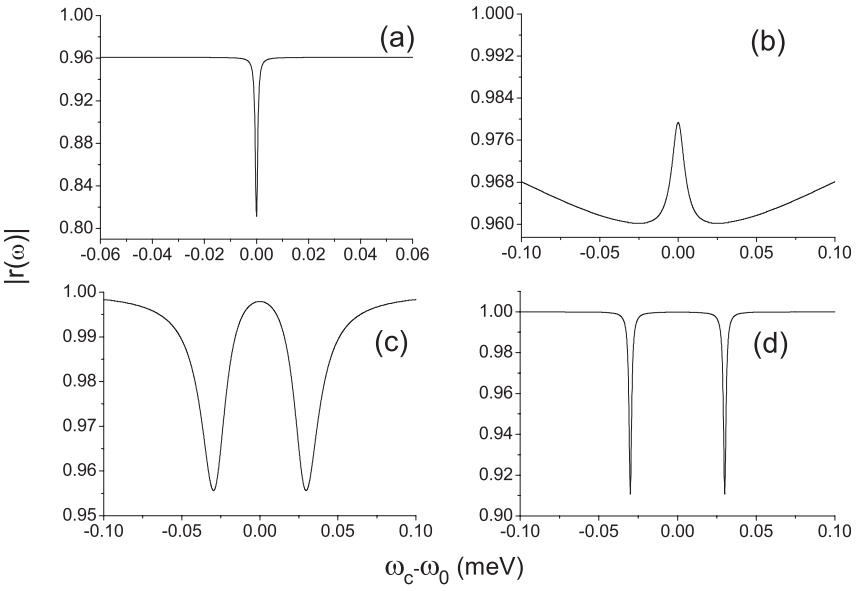

Figure 3. Plots showing the reflection spectra against detuning where $\omega_a = \omega_c$ for (a) $\kappa = 75\,\mu$eV, (b) $\kappa = 7.5\,\mu$eV, (c) $\kappa = 0.75\,\mu$eV, (d) $\kappa = 0.075\,\mu$eV, and $\eta = 50\kappa$ for all of the above.

measures the population inversion. If we now combine this with the input–output relation for this cavity:

$$b_{\text{in}} - b_{\text{out}} = \sqrt{\eta}a, \tag{4}$$

then we can find the reflection coefficient for light input into the cavity via b_{in}:

$$r(\omega) = \frac{b_{\text{out}}}{b_{\text{in}}} = \frac{\left[\mathrm{i}(\omega_a - \omega) + \frac{\gamma}{2}\right]\left[\mathrm{i}(\omega_c - \omega) + \frac{\kappa}{2} - \frac{\eta}{2}\right] + g^2}{\left[\mathrm{i}(\omega_a - \omega) + \frac{\gamma}{2}\right]\left[\mathrm{i}(\omega_c - \omega) + \frac{\kappa}{2} + \frac{\eta}{2}\right] + g^2}, \tag{5}$$

where we have set $\sigma_z = -1$ as is appropriate for the weak excitation limit. At low temperature the zero phonon linewidth is 0.1 μeV [19], we set $g = 0.03$ meV as appropriate for a cavity mode volume of 0.02 μm^3, where the NV has an oscillator strength of $\approx$0.2 given a 13 ns lifetime. It is desirable for the cavity to be critically coupled to the input–output so we will set η to be 50 times faster than κ.

Figure 3 shows the effect of varying κ and η on the reflection coefficient. When κ and η are very low we are in the strong coupling regime with $g \gg \kappa, \eta, \gamma$. This strong coupling rate splits the absorbtion feature into what is known as the Rabi split dressed states with detuning $\pm g$ as seen in figure 3(d). The result of this splitting is that all of the light resonant with the cavity mode is reflected. As we increase κ and η we are no longer able to resolve the two states and cross over into what is known as the one-dimensional atom (or Purcell) regime $\eta + \kappa > g > \gamma$ (figure 3(c) to (d)). In this region, almost all SE is into the fundamental cavity mode due to Purcell enhancement. The result is a small peak in reflectivity on resonance in figure 3(b). As the escape rates increase, the damping by the atomic transition (zero phonon line) plays an increasingly dissipative role as a larger proportion of the radiative decay is into non-cavity modes. As a result the peak becomes a strong dip in reflectance on resonance clearly visible in figure 3(a).

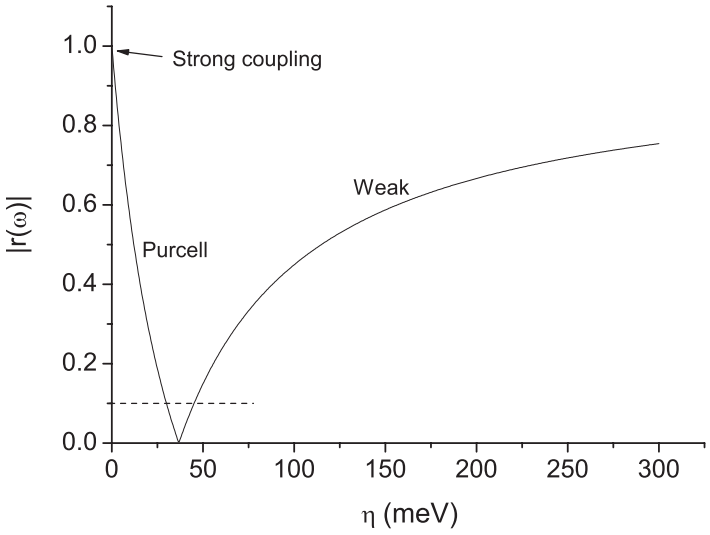

Figure 4. Calculated reflectance against cavity damping at $\omega_c = \omega_a$ and $\omega_c - \omega = 0$, where we have ignored κ as $\eta = 50\kappa$. The relevant atom–cavity coupling regimes are labeled, the strong coupling regime occurs when η is very low and $|r(\omega)| \approx 1$. The crossover from the Purcell regime to the weak coupling regime occurs at a value of 36 meV as predicted. The region below the dashed line is the area we wish to operate.

In figure 4, we have plotted the reflectance at the cavity–atom resonance against η as it is the dominant decay channel for the cavity mode. The amount of reflected light drops to zero at a value of $\eta = 4g^2/\gamma$, which corresponds to the transition from the one-dimensional atom to the weak coupling regime. Thus at this point all of the light absorbed by the NV center is emitted into non-cavity modes. After this turn over point we are in the weak coupling regime, where the NV center has progressively less effect on the dynamics of the system as it so weakly coupled. It is near this transition region, where the reflection coefficient on resonance drops below 10% that we wish to operate, where the narrow feature in the reflection spectrum caused by the zero phonon linewidth dominates (figure 5). This also allows for around a 15% tolerance in the coupling constant η, advantageous when considering possible imperfections in the fabrication processing. It is also worth noting the position of this transition region scales as the inverse of the mode volume (V_{eff}), thus the required Q factor is proportional to V_{eff}. So in order to keep the Q factor low and still be operating in this transition region we need to use a cavity with a small mode volume.

If we consider figure 5, then if we set the cavity to be resonant with the $^3A_{(m=0)}$ to excited state transition then the reflected intensity for resonant excitation with narrow band light becomes:

$$|r(\omega)|^2_{m=0} = \left| \frac{\gamma(\kappa - \eta) + 4g^2}{\gamma(\kappa + \eta) + 4g^2} \right|^2 = 0.001. \tag{6}$$

Almost none of the input light will be reflected when the NV center is in the spin $m = 0$ ground state. However, if it is in the spin $m = +1$ ($m = -1$) state then the 7 μeV (10 μeV) detuning

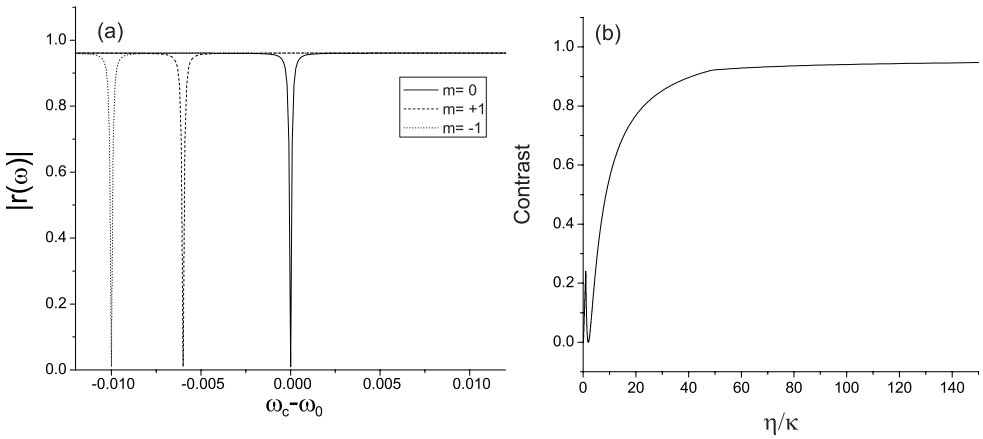

Figure 5. (a) The reflection spectra against detuning where for $\kappa = 750\,\mu$eV, and $\eta = 50\kappa$. There are three spectra corresponding to the three spin levels. All three are coupled to the cavity, which has a linewidth of 37.5 μeV, however, we will only probe the $m = 0$ state with a narrow band laser. (b) Plot showing how intensity contrast $(|r(\omega)|^2_{m=\pm1} - |r(\omega)|^2_{m=0})$ varies with the ratio of η to κ.

means that the NV center is not coupled to our probe field giving a reflected intensity of:

$$|r(\omega)|^2_{m=\pm1} = \left|\frac{(\kappa-\eta)}{(\kappa+\eta)}\right|^2 = 0.92. \tag{7}$$

Nearly all of the input light will be reflected. This contrast in intensity $(|r(\omega)|_{m=\pm1} - |r(\omega)|_{m=0})$ can be easily detected. What makes this result significant is that the curve in figure 5 corresponds to a total Q factor $Q_{\text{tot}} = \omega/(\kappa+\eta) \approx 55$. Since we have set η to be 50 times greater than κ, this means that the photonic crystal cavity before coupling needs to have $Q = \omega/\kappa \approx 3000$. This is much lower than the cavity Q factor of 300 000 that would be required to have the cavity linewidth narrow enough to resolve the two transitions, which when coupled to a waveguide in the same way as here would need to exceed 10^7. It is possible to further reduce the requirements on the cavity Q factor by reducing the ratio of η to κ. However, the result of this is a reduction in the intensity contrast between the two spin states as a larger proportion of the light confined in the cavity leaks out of the side. The intensity contrast which measures the spin is not influenced by total Q factor, the optimal value being $Q_{\text{tot}} \approx 55$, the contrast is only influenced by the ratio of η to κ. It is desirable to have this contrast at a maximum in order to minimize errors in state identification.

There are several benefits to this scheme. The first is the obvious increase in collection efficiency of the photons, making low intensity measurements possible. Since less photons are required to probe the spin state there are less fluorescence cycles therefore a reduced probability of a spin-flip transition. Additionally as the cavity is resonant with the $m = 0$ transition by probing with narrow band light then we never excite the spin ±1 transitions which have a higher probability to spin-flip, hence the system is optimized for spin preserving transitions. However, if we pump with a broad band laser source we can easily spin polarize the ground state to initialize the system. Since we are in the low Q regime then the Purcell factor is small, $F_{\text{p}} \approx 4$ for a system with the parameters listed above, thus the rate of SE into the cavity is not significantly modified. If we were operating in the high Q or strong coupling regime then the

SE rate into the cavity would be much larger, and the decay rate to the ^{1}A singlet state would remain unmodified. Therefore with the probability of a spin-flip transition greatly reduced, the system would not be simultaneously optimized for readout and initialization.

In order to make the scheme experimentally relevant the limitations of current detector technology must be included. If we consider an overall detection efficiency of 33% then if we input 60 photons we can expect to detect 20 with unit reflectivity. If the spin is in the $m = \pm 1$ state ($|r(\omega)|^2 \approx 92\%$) it is reasonable to expect 18 photons to be detected. If the spin is in the $m = 0$ state ($|r(\omega)|^2 < 1\%$) we may expect 1 photon to be detected. If we set a detection threshold of 6 photons the error in the measurement can then be found from the probability of detecting >6 photons when we expect 1 and the probability of detecting < 6 photons when we expect 18, giving an error rate of $\approx 1.5 \times 10^{-3}$ (assuming Poissonian distribution). Standard silicon avalanche photo diodes have a dead time of 50 ns which means that it will take 3 μs to carry out a measurement with 18 detected photons (running at one third of the detector saturation count rate). Since the longest observed spin coherence time of an NV center is 600 μs [28] this introduces a further error rate of 5.5×10^{-3}. There are also errors associated with saturation of the NV center. However, as the detector dead time is much larger than the modified SE lifetime then these are negligible. Finally, there is also an error associated with decay from the $^3E_{m=0}$ to the $^3E_{m=\pm 1}$ state via the ^{1}A singlet state which for 60 photons is $< 10^{-3}$. Thus the total error rate is $\approx 7 \times 10^{-3}$.

Simulations of photonic crystals in diamond have shown Q factors larger than 10^6 for mode volumes around 0.02 μm^3, or larger than 10^5 for mode volumes around 0.008 μm^3 [25]. These values are significantly more demanding than those required for this scheme, particularly the Q factor. Experimental evidence suggests that the actual Q factors will be much lower than those simulated. Cavities fabricated by Wang *et al* [29], showed more than a factor of 10 shortfall in the experimental Q factor compared to the simulated, attributed to defects in the nanocrystalline structure. Nevertheless their measured Q factor of 585 would allow a ratio of $\eta \approx 10\kappa$, in order to have an overall Q factor of 55. This would result in a 65% contrast between the two spin states, increasing the error rate to $\approx 2 \times 10^{-2}$. Theoretical considerations of the absorption in nanocrystalline diamond have predicted a reduction in Q factor from a value of 66 300 to a value of around 1350 for a cavity of mode volume 0.02 μm^3 [30]. For our purposes this would result in a contrast of 85%, where the error rate would be $\approx 1 \times 10^{-2}$. So the scheme is clearly robust and can cope with experimental imperfections. The main difficulty with this scheme, which is true for all schemes, is the positioning of the NV center at the field maximum. If the precision is poor then this can have a detrimental effect on the coupling rate g. This in turn reduces the intensity contrast between the two spin states, which is sensitive to the value of g compared to the zero phonon linewidth γ. There is promise that nitrogen implantation in pure single crystal diamond could hold the key to fabricating suitable devices [31, 32]. The use of single crystal diamond would dramatically reduce the absorption losses caused by defects, so experimental Q factors should be closer to the theoretical predictions. An alternative approach to nitrogen implantation is to register existing NV centers in a scanning confocal microscope. The peak of emission can be determined with precision of order 30 nm by fitting the approximately Gaussian peak. It is then possible to build the photonic crystal cavity and waveguide around them.

In conclusion, we have proposed an efficient low error measurement of the ground state spin of an NV center. For the realistic parameters proposed here we can achieve error rates of around 7×10^{-3}. The setup can easily switch between initialization and readout by switching from a broad to narrow band laser source. Low error readout requires modest Q factors, and

even with current limitations of photonic crystal cavities the error rate could be as low as 2×10^{-2}. Work needs to be done on the design and fabrication of photonic crystal cavities coupled to waveguides, particularly in single crystal diamond to minimize absorption losses. We also note that we can measure the spin with a single photon with 92% fidelity (assuming ideal detection), where fidelity is simply the contrast between the two spin states. Hence, with some modifications the ideas here could be used to remotely entangle two spatially separated NV centers embedded in cavities, which is a subject for further study.

Acknowledgments

We acknowledge support from the UK EPSRC (QIP IRC), and the European Commission under projects IST-015848-QAP and IST-034368 EQUIND and Nanoscience ERA project NEDQIT. J G R was supported by a Royal society Wolfson Merit award.

References

[1] Nielsen M A and Chuang I L 2000 *Quantum Computation and Quantum Information* (Cambridge: Cambridge University Press) p 91
[2] Kimble H J 1994 *Cavity Quantum Electrodynamics* ed P Berman (Boston: Academic) pp 203–66
[3] Langer C *et al* 2005 Long-lived qubit memory using atomic ions *Phys. Rev. Lett.* **95** 060502
[4] Cirac J I and Zoller P 1995 Quantum computation with cold trapped ions *Phys. Rev. Lett.* **74** 4091–4
[5] Calarco T, Datta A, Fedichev P, Pazy E and Zoller P 2003 Spin-based all-optical quantum computation with quantum dots: understanding and suppressing decoherence *Phys. Rev.* A **68** 012310
[6] Duan L-M and Kimble H J 2004 Scalable photonic quantum computation through cavity-assisted interactions *Phys. Rev. Lett.* **92** 127902
[7] Loss D and DiVincenzo D P 1998 *Phys. Rev.* A **57** 120
[8] Leibfried D *et al* Experimental demonstration of a robust, high-fidelity geometric two ion-qubit phase gate *Nature* **422** 412–5
[9] Schmidt-Kaler F, Haffner H, Riebe M, Gulde S, Lancaster G P T, Deuschle T, Becher C, Roos C F, Eschner J and Blatt R 2003 Realization of the Cirac-Zoller controlled-NOT quantum gate *Nature* **422** 408–11
[10] Li X, Wu Y, Steel D, Gammon D, Stievater T H, Katzer D S, Park D, Piermarocchi C and Sham L J 2003 An all-optical quantum gate in a semiconductor quantum dot *Science* **301** 809–11
[11] Jelezko F, Gaebel T, Popa I, Gruber A and Wrachtrup J 2004 Observation of coherent oscillations in a single electron spin *Phys. Rev. Lett.* **92** 076401
[12] Charnock Forrest T and Kennedy T A 2001 Combined optical and microwave approach for performing quantum spin operations on the nitrogen-vacancy center in diamond *Phys. Rev.* B **64** 041201
[13] Jelezko F, Gaebel T, Popa I, Domhan M, Gruber A and Wrachtrup J 2004 Observation of coherent oscillation of a single nuclear spin and realization of a two-qubit conditional quantum gate *Phys. Rev. Lett.* **93** 130501
[14] Childress L, Gurudev Dutt M V, Taylor J M, Zibrov A S, Jelezko F, Wrachtrup J, Hemmer P R and Lukin M D 2006 Coherent dynamics of coupled electron and nuclear spin qubits in diamond *Science* **314** 281–5
[15] Atature M, Dreiser J, Badolato A, Hogele A, Karrai K and Imamoglu A 2006 Quantum-dot spin-state preparation with near-unity fidelity *Science* **312** 551–3
[16] Berezovsky J, Mikkelsen M H, Gywat O, Stoltz N G, Coldren L A and Awschalom D D 2006 Nondestructive optical measurements of a single electron spin in a quantum dot *Science* **314** 1916–20
[17] Tamarat Ph *et al* 2008 Spin-flip and spin-conserving optical transitions of the nitrogen-vacancy centre in diamond *New J. Phys.* **10** 045004
[18] Loubser J H N and Van Wyk J A 1977 Optical spin polarization in a triplet state in irradiated and annealed type 1b diamonds *Diamond Res.* **11** 11

[19] Wrachtrup J and Jelezko F 2006 Processing quantum information in diamond *J. Phys.: Condens. Matter* **18** S807–24
[20] Manson N B, Harrison J P and Sellars M J 2006 Nitrogen-vacancy center in diamond: model of the electronic structure and associated dynamics *Phys. Rev.* B **74** 104303
[21] Jelezko F and Wrachtrup J 2004 Read-out of single spins by optical spectroscopy *J. Phys.: Condens. Matter* **16** R1089–104
[22] Christian K, Sonja M, Patrick Z and Harald W 2000 Stable solid-state source of single photons *Phys. Rev. Lett.* **85** 290–3
[23] Manson N B and McMurtrie R L 2007 Issues concerning the nitrogen-vacancy center in diamond *J. Lumin.* **127** 98–103
[24] Santori C *et al* 2006 Coherent population trapping in diamond N-V centers at zero magneticfield *Opt. Express* **14** 7986–93
[25] Zhang Z and Qiu M 2007 Small-volume waveguide-section high Q microcavities in 2D photonic crystal slabs *Opt. Express* **12** 3988–95
[26] Faraon A, Waks E, Englund D, Fushman I and Vučković J 2007 Efficient photonic crystal cavity-waveguide couplers *Appl. Phys. Lett.* **90** 073102
[27] Walls D F and Milburn G J 1994 *Quantum Optics* (Berlin: Springer) p 91
[28] Neumann P, Mizuochi N, Rempp F, Hemmer P, Watanabe H, Yamasaki S, Jacques V, Gaebel T, Jelezko F and Wrachtrup J 2008 Multipartite entanglement among single spins in diamond *Science* **320** 1326–9
[29] Wang C F, Hanson R, Awschalom D D, Hu E L, Feygelson T, Yang J and Butler J E 2007 Fabrication and characterization of two-dimensional photonic crystal microcavities in nanocrystalline diamond *Appl. Phys. Lett.* **91** 201112
[30] Kreuzer C, Riedrich-Möller J, Neu E and Becher C 2008 Design of photonic crystal microcavities in diamond films *Opt. Express* **16** 1632–44
[31] Greentree A D *et al* 2006 Critical components for diamond-based quantum coherent devices *J. Phys.: Condens. Matter* **18** S825–42
[32] Gaebel T *et al* 2006 Room-temperature coherent coupling of single spins in diamond *Nat. Phys.* **2** 408–13